Available online at www.sciencedirect.com
ScienceDirect
Polymer 48 (2007) 6834–6842
polymer
www.elsevier.com/locate/polymer

The effect of annealing on the melt rheology of ternary PE/PA6/GF composites

Plamen G. Malchev [a,b,*], B. Norder [a], Stephen J. Picken [a,b], Alexandros D. Gotsis [b,c]

[a] *Delft University of Technology, Department of Polymer Materials and Engineering, Julianalaan 136, 2628 BL Delft, The Netherlands*
[b] *Dutch Polymer Institute, P.O. Box 902, 5600 AX Eindhoven, The Netherlands*
[c] *Technical University of Crete, Department of Sciences, 73100 Chania, Greece*

Received 10 July 2007; received in revised form 31 August 2007; accepted 20 September 2007
Available online 25 September 2007

Abstract

Ternary composites have been prepared by simultaneous extrusion of polyethylene (PE), polyamide-6 (PA6) and short glass fibre (GF) reinforcement. Two types of fibres – compatible either to the PA6 or to the PE phase – were used and this led to composites with distinctly different morphology and properties. The PA6-compatible fibres were interconnected by PA6 bridges and formed a continuous network within the matrix, whereas for the PE-compatible fibres such a network was not formed.

The composites were annealed at temperatures above the melting points of both thermoplastic components and the changes of the rheological properties of their melts were monitored using small amplitude oscillatory flow. A substantial increase of the stiffness of the composites containing PA6-compatible fibres was observed after 2 h annealing at 250 °C. This higher level of stiffness was preserved during the consequent cooling down to 120 °C. The effect of strain softening of the melts was studied by applying different strain amplitudes. The results of the rheological study were analysed using a recently developed theoretical model. The analysis confirmed the relation between the changes of the properties and the development of the morphology that was previously found by dynamic mechanical analysis in the solid state.

Keywords: Short fibre reinforced thermoplastic blends; Morphology development; Rheokinetics study

1. Introduction

The preparation of binary polymer blends and/or ternary composites (based on two thermoplastic polymers and solid filler) often results in a material outside thermodynamic equilibrium. Upon reheating (until a liquid state is obtained) and further annealing of such composite materials, their morphology may change [1–10]. The evolution of the morphology can be followed by monitoring the rheological parameters of the composite melt. In fact, this is often applied to monitor the evolution of a system on a molecular scale. For example, viscometry is used to investigate the progress of the polymerisation process in reactive systems, due to the relation between molecular mass and viscosity [11]. Similarly, the degree of curing can be established from elasticity measurements [12]. The measurement of the viscosity or the variation of the stiffness in such cases is known as *rheokinetics*. In a broader sense this method has been used to study changes of the rheological properties in time, regardless of whether they originate from chemical reaction or by the evolution of the morphology.

Rheokinetics in non-reactive systems was used by Persson and Bertilsson [4] to study the morphology evolution of ternary composites comprising of polyethylene (PE)/polyisobutylenes (PIB), or poly(styrene-*co*-acrylonitrile) (SAN)/polyamide-6 (PA6), and aluminum borate whiskers. It was found that the changes of the morphology correlated with the changes of the melt rheology. A diffusion of the whiskers

* Corresponding author. Delft University of Technology, Department of Polymer Materials and Engineering, Julianalaan 136, 2628 BL Delft, The Netherlands. Tel.: +31 15 2788013; fax: +31 15 2784945.
E-mail address: p.g.malchev@tudelft.nl (P.G. Malchev).

0032-3861/$ - see front matter © 2007 Elsevier Ltd. All rights reserved.
doi:10.1016/j.polymer.2007.09.027

from one polymer phase to the other during annealing led to an increase of the dynamic rheological properties.

Ternary composites consisting of PE and PA6 reinforced with short glass fibres (GF) are discussed in the present article. When PA6-compatible fibres are used, the PE/PA6/GF composites develop a complex network that consists of glass fibres interconnected by bridges of the PA6 phase [13]. This effective continuous network improves the mechanical properties of the ternary composites, in comparison with their binary (PE/GF) equivalents; and extends their thermal stability to higher temperatures, even above the melting point of the matrix. Therefore, such ternary composites (short fibre reinforced blends) are good candidates for alternative materials that combine the mechanical properties of continuous fibre composites together with the ease of processing of short fibre reinforced thermoplastics.

Here the evolution of the morphology of the PE/PA6/GF composites during annealing is studied by rheokinetics. The observed effect is an increase of the dynamic moduli (G', G'') of the melt. The underlying mechanism responsible for this increase is the reshaping of the minor-phase domains (i.e. the PA6/GF network).

The morphology evolution of these systems was discussed in a related publication [15], where a dynamic mechanical analysis (DMA) in the solid state (i.e. below the melting of the PA6 component) was used to generate the experimental data, but over a limited time range. In the present rheokinetics study we provide results over longer time scales, that undoubtedly demonstrate an increase in the elastical properties of the ternary composites containing PA6-compatible fibres and their melts. Since longer annealing times are explored here, more accurate determination is made of the time scale at which the morphology changes. This study also clarifies the precise moment, or rather temperature, at which the process begins and associates it to the melting of the dispersed (PA6) phase. Although the general trends observed for the ternary composites by DMA are confirmed by the present analysis, a direct comparison between these two methods is not possible, due to the differences in the test conditions. The various results can, however, all be explained by means of recently developed theoretical models, which correlate the morphology to the strain softening of the melt [14] and the dynamic mechanical properties of the composites [13,15].

2. Materials and experimental part

The ternary composites are compounded of two immiscible thermoplastic polymers and a glass fibre reinforcement. Two low density polyethylenes were used as a matrix polymer. They have about the same melting temperature and tensile modulus, but different viscosities (see Fig. 1). The lower viscosity grade is denoted as PE1 and the higher one as PE2. The second thermoplastic polymer, added at ≤ 15 vol.%, was polyamide-6 (PA6). The properties of the components are given in Table 1. Short glass fibres were used as reinforcement. They were compatible either to the PA6 phase or to the PE phase and are denoted here as GF1 and GF2, respectively. Their

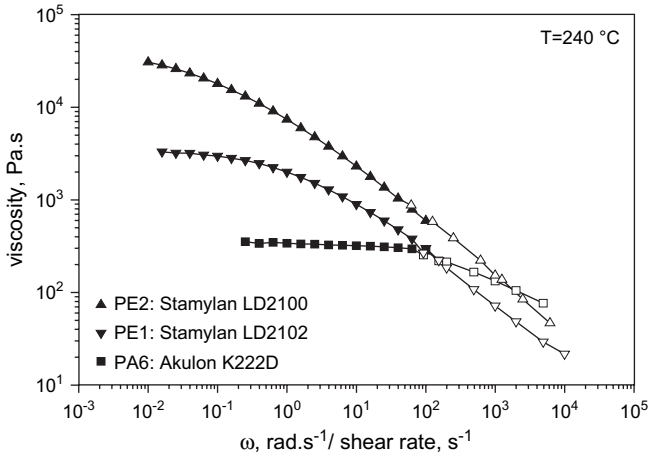

Fig. 1. Viscosity curves of the components measured at 240 °C. Closed symbols: complex shear viscosity as a function of the frequency (oscillatory rheometry). Open symbols: shear viscosity as a function of the shear rate (capillary rheometry).

physical properties are also listed in Table 1. PA6 was dried before use in a vacuum oven for 24 h at 80 °C, whereas the rest of the components were used as delivered.

Following the notations in Ref. [13] the composites are denoted here by the volume fractions of the components (in vol.%) followed by the types of the components. For example, 85/15 PE1/GF2 is a code for a binary composite (mixture) containing 85 vol.% of the lower viscosity polyethylene and 15 vol.% of the PE-compatible fibres; whereas 70/15/15 PE2/PA6/GF1 is a code for a ternary composite (mixture, short fibre reinforced blend) containing 70 vol.% of the higher viscosity polyethylene, 15 vol.% of the PA6 component and 15 vol.% of the PA6-compatible glass fibres.

A co-rotating twin screw extruder (Werner & Pfleiderer ZSK-D28) was used to mix the components. It was operated at low speed (20 rpm) to prevent the breakage of the fibre reinforcement. The temperature of the mixing section was 240 °C (at this temperature both polymeric components are molten) and 260 °C at the exit die (ϕ 2 mm). The extrudates

Table 1
Properties of the components

Code	MFR,[a] dg/min	Melting temp. (°C)	Density, g/cm^3	Modulus, Pa (25 °C)	Trade name
Polymers					
PA6	–	220	1.13	2×10^9	Akulon K222D
PE1	1.9	110	0.921	250×10^6	Stamylan LD2102
PE2	0.3	110	0.921	250×10^6	Stamylan LD2100

Code	Compatible with	$[2r \times l_i]$,[b] μm × mm	Density, g/cm^3	Modulus, Pa (25 °C)	Trade name
Glass fibres					
GF1	PA6	10.0×4.5	2.60	72×10^9	PPG 3545
GF2	PE	13.7×3.0	2.60	72×10^9	PPG 3299

The polymers are commercial grades and were delivered by DSM and SABIC Europe. The glass fibres were delivered by PPG Industries.

[a] Melt flow rate.

[b] (Fibre diameter) × (initial fibre length).

were cooled in water, collected on a rotating roll, dried and kept in a vacuum oven at 80 °C. The homogeneity of the samples was very good, with moderate breakage of the fibres during the processing (fibre length after extrusion, $2l_f \sim 500$ μm). The extrudates were manually arranged, taking care to preserve their parallel alignment (Fig. 2), and compacted into discs (ϕ 25 mm, 2 mm thick) using a hot press at 190 °C for about 15 min. Therefore, the fibres are mostly parallel to the plates of the rheometer. The PA6 component remained frozen and the morphology of the samples was preserved as formed in the extruder. These discs were used for the rheology experiments.

The rheological measurements were conducted in a strain controlled rheometer (Rheometrics RMS 800) operated with plate–plate fixtures (ϕ 25 mm) under nitrogen at 1 Hz. Complete frequency sweeps of these composites are reported in Ref. [16]. Because a plate–plate distance larger than three times the average fibre length is required to avoid wall effects ([17] and references therein) a gap of 2 mm was used.

Two sets of measurements were conducted. In the first set, the morphology evolution was monitored using 0.5% strain amplitude oscillations. For each measurement, the sample was placed in the rheometer at 120 °C and allowed to relax until a zero normal force was achieved. This temperature is about 10 °C higher than the melting point of the matrix polymer (PE) and was the lowest at which plastic deformation of the samples is possible for the precise correction of the rheometer gap. An oscillation of 0.5% strain amplitude was applied for 1 h to ensure the complete sample relaxation and a temperature sweep was started then. The temperature was increased from 120 °C to 250 °C at a rate of 5 °C/min. The final temperature was set 30 °C above the melting point of PA6 to ensure measurable kinetics of the morphology evolution. The changes are viscosity dependent and increase in speed with the decrease of the viscosity at high temperatures. If the temperature is too high, however, a degradation of the polymers will occur. Therefore, 250 °C was the best compromise for conducting the measurements, providing high kinetics of the morphology development and low thermal degradation of the polymers. As it will become clear later, a substantial part of the network development occurs immediately after the melting of PA6, therefore, the temperature was increased in a controlled manner to precisely establish the beginning of the process. After a temperature of 250 °C was reached, the samples were subjected to oscillatory shear under constant temperature for 2 h. This time was considered long enough for obtaining an equilibrium morphology. Then, the samples were cooled down to 120 °C at the same rate. At the end of this cycle, the rim of the sample was removed, and a second heating and cooling cycle was conducted under the same conditions, but with a slightly smaller gap. This cycle was performed to confirm that no further morphology developments will take place. A full record of the temperature cycles is shown in Fig. 3.

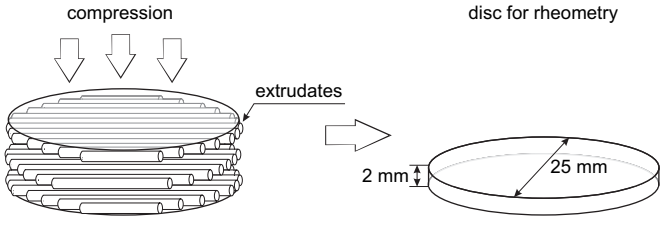

Fig. 2. Schematic representation of the arrangement of the extrudates within the rheometry samples.

A second set of experiments were used to examine the effect of the strain amplitude on the changes of the moduli during the annealing. During these experiments, the rheometer was conditioned at 250 °C, the gap was set to 2 mm and oscillations with 0.1%, 0.3%, 0.5%, 1%, 3%, and 7% strain amplitude were started. The total annealing time was again 2 h.

We note that the sedimentation of the fibres within the time frame of these experiments can safely be neglected. The sedimentation time, τ_s, is defined as the time required for a vertical fibre to fall over its full length [18]:

$$\tau_s = 4\eta_m l_f / \{\Delta\rho g r^2 [\ln(2l_f/r) - 0.72]\},$$

where η_m is the viscosity of PE, $2l_f$ is the (average) length of the fibres after the extrusion, $2r$ is their diameter, g is the acceleration of gravity and $\Delta\rho$ is the density difference between glass and PE. Taking into account that the densities of the glass fibres and PE are, respectively, 2.60 g/cm^3 and 0.921 g/cm^3 for the melts studied here, $\tau_s \approx 30$ h.

3. Results and discussion

Fig. 3 shows the variation of the storage modulus, $G'(t)$, and the temperature, $T(t)$, during the first measurement cycle. Several binary and ternary composites were tested. Plot (A) includes the curves of ternary composites containing the same volume fractions of the components but either the lower (PE1) or the higher viscosity (PE2) matrix. Plot (B) includes the data of two binary composites (85/15 PE1/GF1 and 85/15 PE1/GF2) containing PA6- or PE-compatible fibres, respectively. Plot (C) is a magnification of the data in plot (A) in the time range of 5000–10,000 s. Plot (D) shows two runs for the 70/15/15 PE1/PA6/GF2 composite to illustrate the reproducibility.

3.1. Composition dependence of the modulus increase during annealing

The main observation made during the annealing of the composites is that their storage modulus increases (in the 3rd time intervals in the plots of Fig. 3). For the binary composites and for the ternary composites containing GF2 this increase is very small and can be associated with the slow cross-linking of the PE matrix at sufficiently high temperatures [4]. The cross-linking of PE is seen in this figure as a monotonous increase of the modulus, with a slope between 0.2 and 0.4 Pa/s. The modulus increase for the ternary composites containing GF1, however, is significant and cannot be explained by the thermal cross-linking of PE. For these

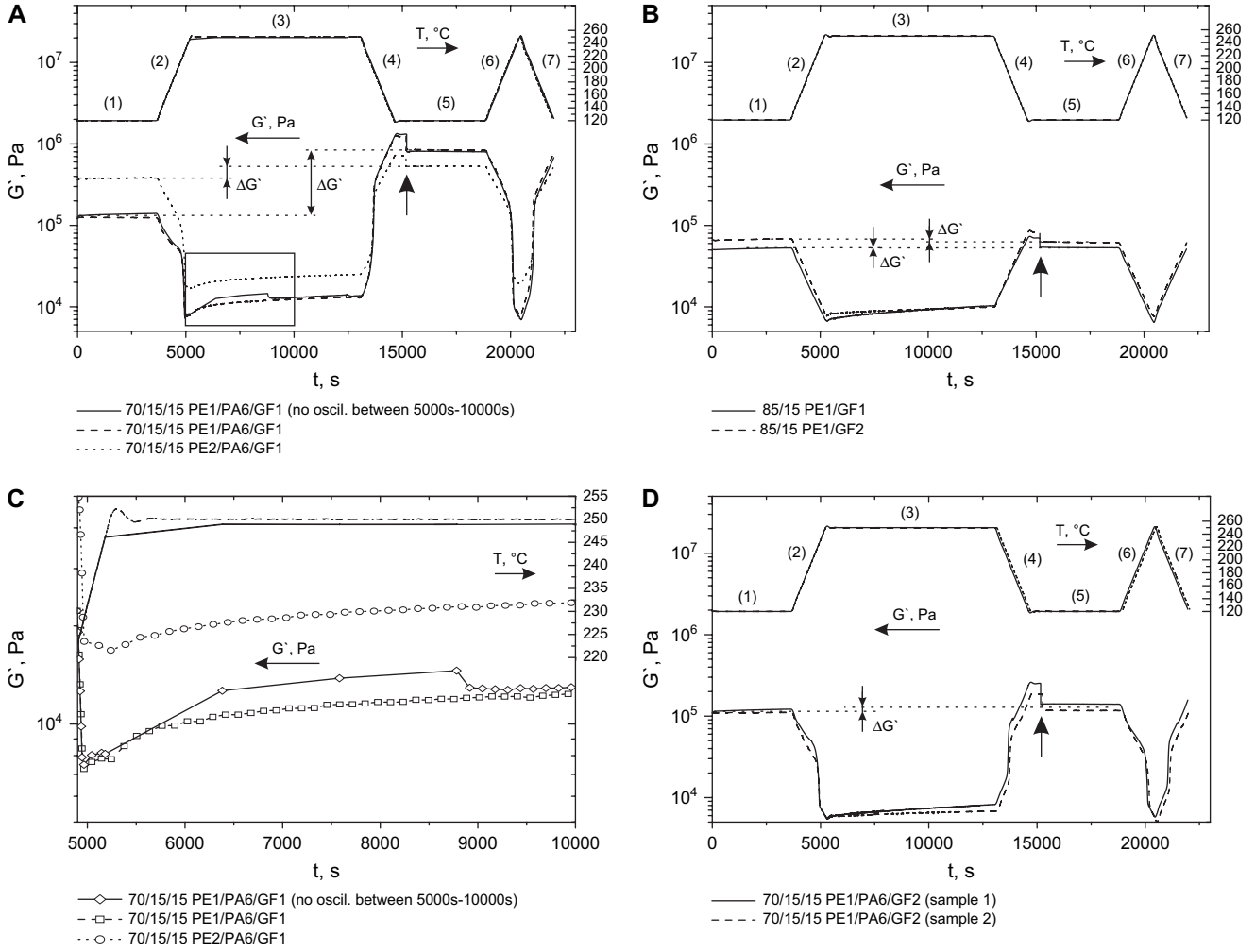

Fig. 3. Temperature and storage modulus (G') vs. time. (A) G' of ternary composites of lower and higher viscosity matrix and PA6-compatible fibres annealed for 7200 s. (B) G' of binary composites. (C) Influence of the oscillating strain (amplitude 0.5%) on G'. (D) Ternary composites of PE-compatible fibres show a negligible modulus increase during the annealing. *Temperature stages*: (1) initial sample conditioning at 120 °C; (2) first heating cycle (120–250 °C, rate 5 °C/min); (3) annealing at 250 °C for 7200 s; (4) first cooling to 120 °C (5 °C/min); (5) new conditioning at 120 °C for 3600 s; (6) second heating cycle; and (7) second cooling cycle. The arrows (in the 5th region) point at the resetting of the gap. $\Delta G'$ indicates the modulus increase at 120 °C realised during the annealing at 250 °C.

composites, it was proposed that an effective network of fibres welded by the minor PA6 phase is formed during the extrusion [13]. The increase of the storage modulus is a consequence of the morphological changes (coarsening of the network) that take place. In the course of annealing more PA6 is attached to the crossing or contact points of the fibres, which leads to the improvement of the PA6/GF network and to an increase of the storage modulus of the system. The coarsening is driven by the reduction of the interfacial energy of the short fibre reinforced blend.

This strong increase of the storage modulus is shown in Fig. 3(A) and (C). The samples containing the lower viscosity matrix show a stronger relative increase [Fig. 3(C) – note the logarithmic scale of the vertical axis]. The increase of the modulus is enhanced by the PA6 crystallisation when the samples are cooled down to 120 °C (just above the PE melting temperature). At this temperature there is a large difference between the behaviours of the homologous ternary (70/15/15 PE1/PA6/GF1) and binary (85/15 PE1/GF1) composites, Fig. 3(A) and (B), respectively. The ternary composites that contain the PA6/GF network reveal solid-like behaviour ($G' > G''$) with very high values of the storage modulus, whereas their binary equivalents are liquid-like ($G' < G''$). This difference is due to the presence of the network [13]. The wettability of the fibre surface by the minor component is found to be crucial for the formation of the network. Matrix compatible fibres (GF2) are incapable to form a strong network, as they are not wetted by the PA6 component. Therefore, no substantial modulus increase is achieved in the case of binary composites or ternary composites containing GF2 (Fig. 3(B) and (D)).

3.2. Influence of the monitoring oscillations

The increase of the storage modulus of the GF1 ternary composites may be caused by two factors: (i) network coarsening, leading to increased stiffness of the network junctions and (ii) the creation of new junction points. The application of

a continuous oscillatory deformation on the sample may lead to the rearrangement of the fibres and to the formation of new contacts between them, causing an increase of the modulus. The influence of the applied oscillation may be significant.

To study this influence, two identical samples were subjected to the same temperature cycle; in one of them the oscillation was continuous, in the other it was intermittent – with short duration around three measurements. In Fig. 3(A) and (C) the latter run is denoted as "*no oscillations between 5000–10,000 s*". Contrary to the expectations, the increase of the storage modulus was somewhat larger during the intermittent testing of the sample. When the oscillations were resumed at $t = 8800$ s, a relaxation process took place that brought the modulus down to the same value as for the continuously tested sample, Fig. 3(C). This indicates that the application of small amplitude oscillations had no major influence on the development of the morphology, and all long term changes originate from an interfacial tension driven evolution of the system.

3.3. Normalisation of the modulus curves

Fig. 4 shows the storage moduli of the composites as functions of temperature, before and after their annealing. The plots correspond to the two heating cycles, stages (2) and (6) of Fig. 3, respectively. The $G'(T)$ curves in Fig. 4 are a result of the simultaneous action of three factors: (i) the effect of the temperature on the stiffness of the components (during the heating); (ii) the development of the network structure (that occurs after the PA6 melting); as well as (iii) the slow thermal cross-linking of the PE matrix (substantial at long annealing times). In order to establish the relation between the morphology and the properties, a renormalisation is necessary, where the extra contributions are subtracted and only the effect of the annealing on the network remains.

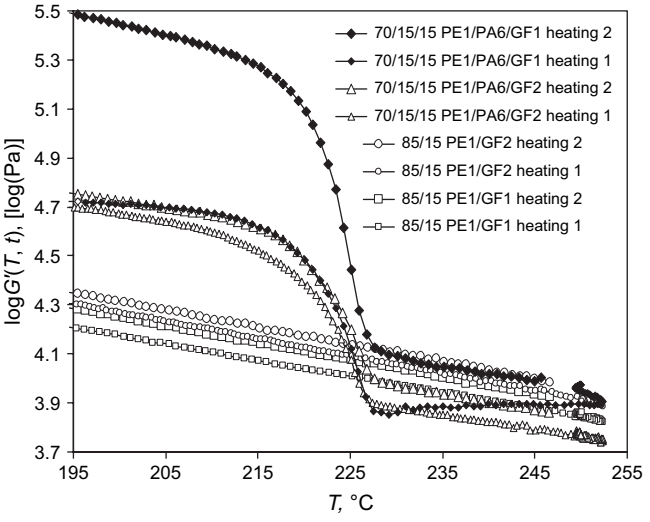

Fig. 4. Temperature sweeps at 5 °C/min. The logarithm of the storage modulus, log G', of different ternary and binary composites is shown before and after annealing, indicated as (heating 1) and (heating 2), respectively. These two cycles correspond to stages (2) and (6) of Fig. 3.

3.3.1. Temperature correction of the modulus

The moduli of the binary composites (85/15 PE1/GF1 and 85/15 PE1/GF2) decrease steadily with increasing temperature in Fig. 4. The slopes of the curves (in a logarithmic plot) are the same for both composites during both heating cycles. The decrease can be attributed to the softening of the PE matrix melt with increasing temperature. For each of these composites the values of the modulus measured before and after the annealing are about the same.

The modulus of the ternary composites, 70/15/15 PE1/PA6/GF1 and 70/15/15 PE1/PA6/GF2, drops rapidly around 220 °C, the melting of the PA6 phase. The two curves above this temperature, however, are very different. The modulus of the composite with PE-compatible fibres (GF2) decreases with the same slope as the binary composites, and follows about the same curve before and after annealing. The modulus of the composite prepared with PA6-compatible fibres (GF1) increases with temperature above 227 °C. After annealing at 250 °C for 2 h the storage modulus of this composite increased dramatically. The enhancement of the modulus at 120 °C is 7.7 times and at 195 °C it is 5.8 times.

Upon increasing the temperature above the melting point of PA6 in the second heating cycle the modulus (of the GF1 containing composite) does not repeat its behaviour from the first heating cycle. Instead, it decreases with the same slope as the one observed for the rest of the samples. This altered behaviour suggests that the morphological changes that involve the restructuring of the PA6/GF network start immediately after the melting of PA6 in the first heating cycle and are completed during the annealing process.

In fact, a substantial part of the network development takes place during the heating of the material from 230 °C up to the annealing temperature, $T_a = 250$ °C. If there were no morphological changes taking place during the first heating cycle, the modulus should have followed the same behaviour as the one demonstrated after the annealing, i.e. a steady decrease. In reality, however, the softening of the matrix is compensated by the stiffening of the network. Therefore, if the $G'(T, t)$ curve beyond the PA6 melting is renormalised by subtracting the common linear slope (on a logarithmic plot) a purely time dependent storage modulus, $G'_{T_a}(t)$, can be obtained that is correlated to the morphological changes and matrix degradation (cross-linking) only:

$$\log G'_{T_a}(t) = \log G'(T,t) - c_T\left[T(t) - T_a\right]/\ln(10), \qquad (1)$$

$$\text{e.g., } G'_{T_a}(t) = G'(T,t)\mathrm{e}^{-c_T[T(t)-T_a]},$$

where T_a is the reference temperature for the renormalisation of the modulus (i.e. the annealing temperature), $T(t)$ represents the temperature at time t, and the averaged slope c_T is 15.8×10^{-3} [1/K] for the PE1 containing composites and 11.5×10^{-3} [1/K] for the PE2 composites. Eq. (1), applied to the 70/15/15 PE1/PA6/GF1 composite, discloses the substantial modulus enhancement taking place during the first heating cycle. Note that this time dependence is not observed during the second heating cycle and is also absent for the

modulus of the binary composites or the ternary composite containing GF2, Fig. 5.

In fact, applying Eq. (1) to the experimental data points transposes them to a temperature $T_a = 250\,^{\circ}C$. In this relation since the morphological changes for the GF1 containing composite start already at a temperature of 227 °C (Fig. 4) the application of Eq. (1) results in an effective modulus, which will be measured for this sample if one can place it immediately at the annealing temperature of 250 °C without any morphological changes to be allowed. Obviously, such state is not practically achievable, but its characteristics can be extracted correcting the experimental data throughout the complete measurement cycle via Eq. (1).

3.3.2. Modulus correction for the degradation (cross-linking) of the matrix PE

After applying Eq. (1), the data measured during stage (2) in Fig. 3 at temperatures above 227 °C and during the subsequent annealing in stage (3) merge. Thus, the annealing process in fact starts earlier, immediately after a temperature of 227 °C is reached, at a reference time $t_{ref} \approx 4980$ s. The linear time increase of the modulus caused by the cross-linking of PE at long annealing times can be subtracted in order to find the renormalised curve of the modulus, $G'_{T_a}(t_a)$:

$$G'_{T_a}(t_a) = G'_{T_a}(t') - D_g(t' - t_{ref}), \tag{2}$$

where $t_a (= t' - t_{ref})$ is the renormalised annealing time and $D_g = 0.2–0.4$ Pa/s is the degradation (cross-linking) rate. The curves of $G'_{T_a}(t_a)$ correspond now only to the evolution of the network structure.

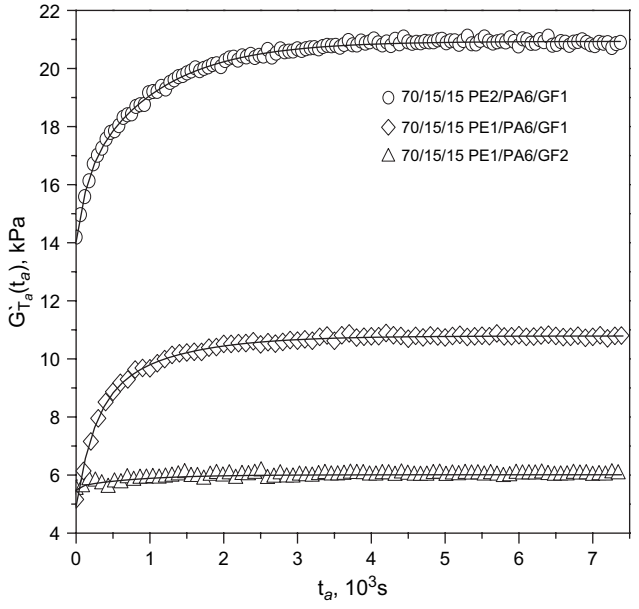

Fig. 5. Corrected storage modulus. The data include part of the temperature sweep (stage 2) and the subsequent time sweep (stage 3) from Fig. 3. The lines are fits of Eq. (3).

3.4. Dynamics of the morphological changes during the annealing

Fig. 5 shows the curves of $G'_{T_a}(t_a)$ of the ternary composites obtained after the corrections, Eqs. (1) and (2). The modulus of the composite containing GF2 is almost constant. In contrast, the moduli of the ternary composites containing GF1 increase during annealing. For the 70/15/15 PE1/PA6/GF1 composite the ultimate increase is 120%. For the 70/15/15 PE2/PA6/GF1 this is around 50% and also the change proceeds more slowly.

The shape of the $G'_{T_a}(t_a)$ curves can provide further information. We find that these curves can be described by the sum of two Debye processes:

$$G'_{T_a}(t_a) = G'_0 + G'_1\left(1 - e^{-t_a/\tau_1}\right) + G'_2\left(1 - e^{-t_a/\tau_2}\right), \tag{3}$$

where G'_0 is the initial storage modulus normalised to the annealing temperature ($T_a = 250\,^{\circ}C$), and (G'_1, τ_1) and (G'_2, τ_2) are the amplitudes and the time constants of the two processes. The maximum (equilibrium) value of the modulus is $G'_{t_a \to \infty} = G'_0 + G'_1 + G'_2$. The experimental data were fitted to Eq. (3) (Fig. 5) and the obtained parameters are listed in Table 2.

The first process is dependent on the matrix viscosity (Table 2). We assume that it is related to the process of creation of new network contact points. During the extrusion of the composites the dispersed phase is forced towards the surface of the fibres, where it forms thin layers. The thickness of the layers is determined by the viscosity ratio of the two thermoplastic components and by the interfacial energies of all interfaces. Increasing the viscosity of the matrix and improving the affinity of the dispersed phase towards the fibrous reinforcement leads to the formation of thicker layers [19]. Such annular liquid layers are generally unstable [15,20–25]. Therefore, upon reheating and remelting the PA6 layers will start break-up and form beads on the surface of the fibres. This process increases the effective radius of the fibres and provides with suitable conditions for the formation of new contact points. The rate of the break-up process, Q_m (and, respectively, of formation of new contacts), depends on the viscosity of the liquid, forming the layer, and is strongly influenced by the thickness of this layer (e.g. [20]):

$$Q_m \approx \frac{\Gamma\left(1 - k_m^2 r^2\right) k_m^2 h^3}{3\eta_0 r^2}, \tag{4}$$

for $h \ll r$ and $\rho Q_m h^2/\eta_0 \ll 1$. The parameters appearing in Eq. (4) are the following: Γ is the interfacial tension; $2\pi/k_{max} \gg 2\pi(r + h)$ determines the wave length of the dominant instability responsible for the break-up of the liquid annular layer; η_0 and ρ are the zero shear rate viscosity and the density of the film forming liquid, respectively; r is the fibre radius; and h is the film thickness. Obviously, higher viscosity and thinner layers slow down the process. The viscosity of the surrounding media (in our case the PE melt) should also have an influence. Although there is not a theoretical interpretation accounting for it, one can expect that the increase of the matrix viscosity slows down the process. In analogy to Rayleigh

Table 2
Parameters obtained by fitting Eq. (3) to the experimental data

Composite	G'_0, Pa	G'_1, Pa	τ_1, s	G'_2, Pa	τ_2, s	$G'_{t_a\to\infty}$, Pa
70/15/15 PE1/PA6/GF1	4930 ± 30	3291 ± 90	239 ± 8	2568 ± 95	996 ± 27	10,789
70/15/15 PE2/PA6/GF1	14034 ± 34	1975 ± 43	143 ± 6	4926 ± 38	1027 ± 8	20,935
70/15/15 PE1/PA6/GF2	5483 ± 32	121 ± 32	50 ± 25	407 ± 14	836 ± 37	6011

instability of a liquid jet placed in a viscous media [26], this is expected to be a relatively weak dependence. Therefore, since in the case of lower viscosity matrix (i.e. PE1) thinner layers are formed [15], the process of creation of new contact points for this composites will take longer time compared to the composites containing higher viscosity matrix (i.e. PE2), as also revealed by Table 2. The second, slower, process is attributed to the morphological changes driven by the need for migration of the PA6 phase towards the newly formed or already existing network junction points. Such process additionally minimises the interfacial energy of the system and is mostly governed by the viscosity of the PA6 phase. The process is found slightly slower for the higher viscosity matrix (Table 2), as can be expected. The magnitude of both processes is much smaller in the case of the GF2 composites, due to the absence of the network structure.

The SEM picture of a fractured surface reveals the presence of the thin PA6 layer surrounding the fibres before the annealing, Fig. 6 (left). This intrinsically unstable morphology is frozen by quenching the extrudates. The layer melts during the subsequent annealing, and breaks into beads on the fibre surface via *Rayleigh instability of an annular liquid layer surrounding a cylindrical surface*. The interfacial energy of the system is minimised further by the accumulation of PA6 at the points where the fibres come close together or intersect, Fig. 6 (the image on the right). Some additional proof (an optical micrograph) confirming this scenario can be found in Ref. [15].

3.5. Influence of the strain amplitude

The melts of the ternary composites containing GF1 are found to be highly strain softening. A recent theoretical model [14] links the degree of softening to the morphology of the melts, and attributes it to the presence of capillary forces acting between the fibres. These forces arise from the deformation of the PA6 bridges, which in the model for simplification are assumed to be cylindrical and to have an initial length L_0 and radius a_0 (Fig. 7). In the present article we apply this model to describe the variation of the bridge radius, $a_0(t_a)$, during annealing, in order to further investigate the evolution of the composite morphology.

The model implies that the application of an external deformation on the sample results in stress localisation in the weakest links of the network, the smallest bridges that are present in the system. These bridges experience the largest local deformations and the variation of their interfacial energy is responsible for the strain softening. The equation proposed in Ref. [14] for the strain dependence of the shear modulus of a ternary PE/PA6/GF composite is:

$$G'(\gamma) = G'_{\mathrm{p}}\left(\frac{-k}{\gamma(1+k\gamma)^2} + \frac{k}{\gamma\sqrt{1+k\gamma}}\right) + G'_{\mathrm{s}}(\gamma), \tag{5}$$

where γ is the external strain; k is a parameter that shows the magnification of the local strain with respect to the externally applied strain amplitude; G'_{s} is the storage shear modulus of the system without the contribution of the bridges; and $G'_{\mathrm{p}} = (2/3)[G'_0 - G'_{\mathrm{s}}(0)]/k^2$, where G'_0 is the zero strain modulus of the ternary blend. $G'_{\mathrm{s}}(\gamma)$ can be extrapolated from the region of high strains or can be assumed to be equal (within a constant) to the modulus of the equivalent binary system that contains the same amount of fibres without PA6. The parameter k is related to the length ($2l_{\mathrm{f}}$) of the fibres: $k \sim l_{\mathrm{f}}/(2L_0)$. For the 70/15/15 PE1/PA6/GF1 composite its value was found to

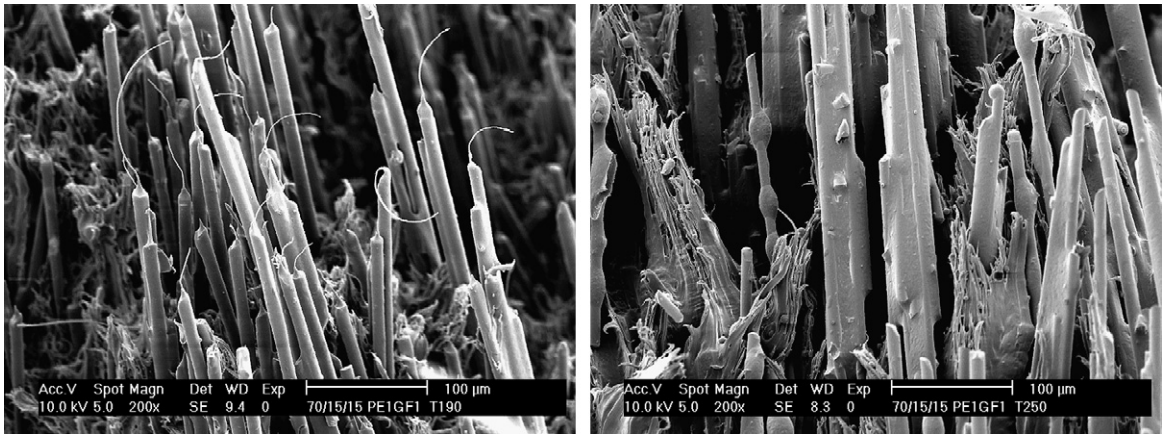

Fig. 6. Morphology development in the 70/15/15 PE1/PA6/GF1 composite during annealing. SEM images of fractured surfaces. Fibres are coated with a thin PA6 layer during the extrusion (left). After annealing at 250 °C, droplets of PA6 are formed on the fibre surface (right).

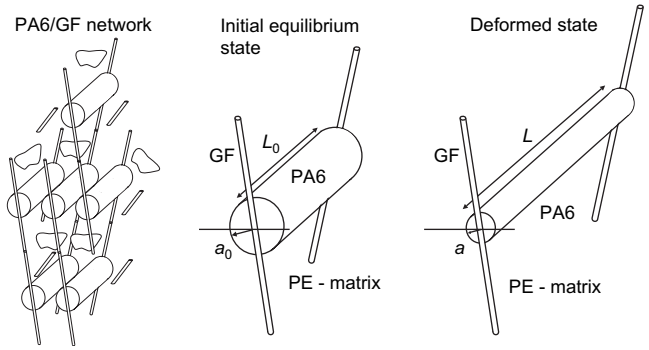

Fig. 7. Schematic of the PA6/GF network for the strain softening model. Initial state of a bridge contributing to the strain softening mechanism and its deformation after the application of the external strain.

be [14]: $k = 121 \pm 7$; and this value is used here to fit the experimental data at different annealing times. The value of G'_p is expressed as:

$$G'_p = (\pi n_a \Gamma L_0 / V_{tot}) a_0, \quad (6)$$

where n_a is the number of (weak) bridges contributing to the strain softening; Γ is the interfacial energy of the PE/PA6 interface; and V_{tot} is the total sample volume. Assuming that the number and the initial length of the weak bridges are preserved constant during the annealing, G'_p is expected to vary with the annealing time via $a_0(t_a)$.

The correspondence between the degree of softening and the microstructure of the composites allows one to extract information about the morphology development by performing strain sweeps at different annealing times, or by performing annealing experiments at different strain amplitudes. Therefore, six samples of the composition 70/15/15 PE1/PA6/GF1 were tested during annealing by oscillations of different amplitudes (Section 2). The data for the storage modulus were subsequently corrected according to Eqs. (1) and (2), and this is shown in Fig. 8. Due to the strain softening, the

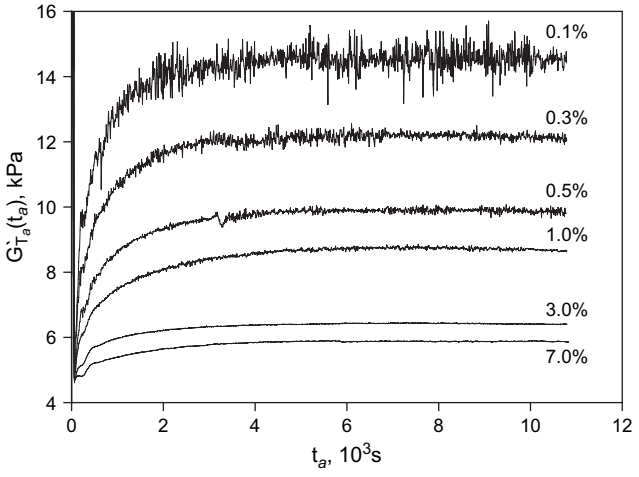

Fig. 8. Impact of the strain amplitude on the storage modulus measured during the annealing. The data have been corrected according to Eqs. (1) and (2).

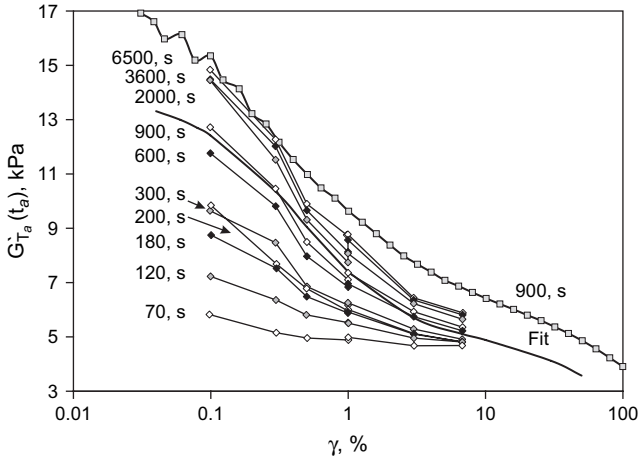

Fig. 9. Strain softening of 70/15/15 PE1/PA6/GF1 composites at different annealing times as extracted from Fig. 8. The solid line is the fit of Eq. (5) through the points obtained after 900 s annealing. For comparison the top curve is a strain sweep measurement conducted after 900 s annealing replotted from Ref. [14].

equilibrium value of the storage modulus decreases with increasing strain amplitude.

Fig. 9 shows the corrected storage modulus as a function of the strain amplitude after various annealing times t_a, as extracted from Fig. 8. These curves are fitted to Eq. (5) and values of $G'_p(t_a)$ are obtained. Next, utilising Eq. (6) the radius of the weak PA6 bridges, contributing to the softening, can be evaluated at any annealing time, $a_0(t_a)$, if the number of weak bridges is known. This number (n_a), however, is inaccessible experimentally. Therefore, the value of n_a was estimated assuming that the average initial radius of the weakest links is

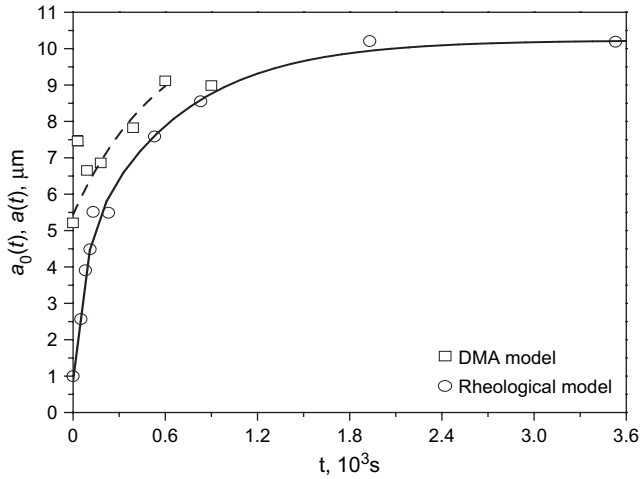

Fig. 10. The time evolution of the radius of the weakest junction points, $a_0(t)$, obtained after fitting the data from Fig. 9 to the strain softening model, Eqs. (5) and (6). The initial radius of the cylinders is chosen to be 1 μm to ensure that the final radius of the weakest junction points does not exceed the average size, $a(t \to \infty)$, obtained by fitting the DMA data with the mechanical model [15]. The solid line is a fit with the sum of two Debye processes. Their time constants are (69 ± 42) s and (637 ± 206) s, respectively. The amplitude of the faster process is about 1/3 of the slower one.

in the order of 1 μm. This value ensures that the final radius obtained by the weak bridges during their annealing does not exceed the average value obtained from the DMA experiments of Malchev et al. [15]. The comparison of the values of the radii of the PA6 domains obtained by the two methods is shown in Fig. 10. The increase of the radius can be fitted again by the sum of two Debye processes with time constants of 69 s and 637 s, respectively. These are smaller than the constants obtained by fitting the storage modulus directly (Table 2). The increase of the storage modulus, however, reflects the increase of the PA6 content at all junction points present in the sample. The strain softening model, on the other hand, mainly probes the evolution of the weak network points, represented by the smallest PA6 cylinders. Naturally, the growth of the smaller PA6 domains connecting two fibres is faster, since they are farther away from thermodynamic equilibrium than the larger domains.

4. Conclusions

In contrast with co-continuous binary blends, where the mechanical properties often deteriorate with the coarsening of the structure, in the ternary PE/PA6/GF composites investigated in the present article the coarsening of the morphology leads to the improvement of the elasticity of the material. The stiffening is observed only for the ternary composites containing PA6-compatible glass fibres and indicates that the driving force for the process is the minimisation of the total interfacial energy of the system. In this respect, two processes can be recognised as important: (i) the process of Rayleigh instability of an annular liquid layer surrounding a fibre surface; and (ii) the process of PA6 accumulation at the points where the fibres come close to each other or intersect.

The evolution of the morphology was successfully monitored by means of rheokinetics measurements. The application of small amplitude oscillatory deformations had no direct influence on the morphological evolution. The morphological changes in quenched samples started immediately after the melting of the PA6 phase. The evolution of the storage modulus was governed by two Debye processes. The saturation of the modulus was achieved after 900 s for the lower viscosity matrix and 1400 s for the higher viscosity matrix. Therefore, composite samples with improved elastic properties can be obtained if they are annealed above the melting temperature of the dispersed phase (PA6 component) for a short period of time.

Acknowledgments

This research forms part of the research programme of the Dutch Polymer Institute (DPI), Project #256. The authors acknowledge PPG Industries for the delivery of the glass fibres and SABIC Europe for the supply of the PE grades.

References

[1] Quintens D, Groeninckx G, Guest M, Aerts L. Polymer Engineering and Science 1990;22(30):1474–83.
[2] Quintens D, Groeninckx G, Guest M, Aerts L. Polymer Engineering and Science 1990;22(30):1484–90.
[3] Verhoogt H. Morphology, properties and stability of thermoplastic polymer blends. Ph.D. dissertation. Delft: Technical University of Delft; 1992.
[4] Persson AL, Bertilsson H. Polymer 1998;39(18):4183–90.
[5] Willemse RC. Polymer 1999;40(8):2175–8.
[6] Veenstra H, van Dam J, Posthuma de Boer A. Polymer 1999; 40(5):1119–30.
[7] Veenstra H, Verkooijen PCJ, van Lent BJJ, van Dam J, Posthuma de Boer A, Nijhof AHJ. Polymer 2000;41(5):1817–26.
[8] Yuan Z, Favis BD. AIChE Journal 2005;51(1):271–80.
[9] Si M, Araki T, Ade H, Kilcone ALD, Fisher R, Sokolov JC, et al. Macromolecules 2006;39(14):4793–801.
[10] Zhang C, Wang P, Ma C, Wu G, Sumita M. Polymer 2006;47(1):466–73.
[11] Cioffi M, Gazeveld KJ, Hoffmann AC. Polymer Engineering and Science 2002;42(12):2383–92.
[12] Malkin AY, Kulichikhin SG. Advances in Polymer Science 1991; 101:217–57.
[13] Malchev PG, David CT, Picken SJ, Gotsis AD. Polymer 2005; 46(11):3895–905.
[14] Malchev PG, Norder B, Picken SJ, Gotsis AD. Journal of Rheology 2007;51(2):235–60.
[15] Malchev PG, de Vos G, Norder B, Picken SJ, Gotsis AD. Polymer 2007;48(12):6294–303.
[16] Malchev PG. Short glass fibre reinforced thermoplastic blends. Ph.D. thesis. Delft University of Technology; 2008.
[17] Sepehr M, Carreau PJ, Moan M, Ausias G. Journal of Rheology 2004; 48(5):1023–48.
[18] Chaouche M, Koch DL. Journal of Rheology 2001;45(2):369–82.
[19] Li C, Zhang Yo, Zhang Yi, Zhang C. Polymers & Polymer Composites 2002;10(8):619–26.
[20] Dumbleton HJ, Hermans JJ. Industrial & Engineering Chemistry Fundamentals 1970;9(3):466–9.
[21] Carrol BJ, Lucassen J. Journal of Chemical Science, Faraday Transactions 1974;70:1228–39.
[22] Rosenau P, Oron A. Physics of Fluids A 1989;1(11):1763–6.
[23] Deissler RJ, Oron A, Lee YC. Physical Review A 1991;43(8):4558–61.
[24] Yarin AL, Oron A, Rosenau P. Physics of Fluids A 1993;5(1):91–8.
[25] Kliakhandler IL, Davis SH, Bankoff SG. Journal of Fluid Mechanics 2001;429:381–90.
[26] Tomotica S. Proceedings of Royal Society A 1935;150:322–37.